Available online at www.sciencedirect.com
SCIENCE DIRECT®
ELSEVIER
Physica B 338 (2003) 16–23
PHYSICA B
www.elsevier.com/locate/physb

Coupling of the effective properties of a random mixture through the reconstructed spectral representation

Elena Cherkaev[a,*], Dali Zhang[a,b]

[a] Department of Mathematics, University of Utah, 155 South 1400 East, JWB 233, Salt Lake City, UT 84112-0090 USA
[b] Department of Mathematics, Harbin Institute of Technology, Harbin 150001, China

Abstract

The spectral representation of the effective complex permittivity of a two-component composite medium is used to develop an approach to coupling of various effective properties of a random mixture. The spectral function contains all information about the microstructure, hence providing a coupling link between the various effective properties of the same composite material. It is demonstrated that the representation can be reconstructed from measurements of one effective property and used then to evaluate other properties of the same material. The reconstruction problem is very ill-posed and requires regularization. Several numerical examples of reconstruction of the spectral function from broadband measurements of the effective complex permittivity and the measurements of the effective thermal conductivity are shown. The approach can be used for indirect estimation of the thermal conductivity (or other properties) of the medium from broadband measurements of the effective complex permittivity.

Keywords: Spectral representation; Random mixture; Broadband measurements; Coupling; Effective properties; Stieltjes function

1. Introduction

Different effective properties of finely structured heterogeneous mixture are coupled through its microgeometry. Formalization of this coupling is very important for predicting properties of composite materials in material design, as well as for indirect evaluation of the effective properties—when direct measurements are difficult to make. Implicit accounting for the geometry of the composite was started in the pioneering work of Prager [1] in deriving coupled bounds on the effective material properties. Coupled or cross-property bounds use measurements of one effective property to improve bounds on other effective properties. The work of Prager was followed by a number of papers by different authors Avellaneda, Berryman, Cherkaev, Gibiansky, Milton, Torquato, and others (see references in monographs [2–4]). Various empirical relations or relations derived for specific geometries are used in practice, such as for instance, Kozeny–Carman or Katz–Tompson relations providing an estimate for permeability of a porous material which can be linked to electrical conductivity and other properties of a composite [5,6]. The present work uses explicit analytic representation of various effective properties of a composite through its geometric

*Corresponding author.
E-mail addresses: elena@math.utah.edu (E. Cherkaev), dzhang@math.utah.edu (D. Zhang).

0921-4526/$ - see front matter © 2003 Elsevier B.V. All rights reserved.
doi:10.1016/S0921-4526(03)00452-6

structural function associated with the spectral measure μ in the Stieltjes analytic integral representation of the effective complex permittivity ε^*. This analytic integral representation of the effective permittivity ε^* of a mixture of two materials with permittivity ε_1 and ε_2 was developed by Bergman, Milton, and Golden and Papanicolaou [7–11] in the course of computing bounds for the effective permittivity of an arbitrary two component mixture. The integral representation gives a function $F(s)$ as an analytic function outside the $[0, 1]$-interval in the complex s-plane:

$$F(s) = 1 - \frac{\varepsilon^*}{\varepsilon_2} = \int_0^1 \frac{\mathrm{d}\mu(z)}{s - z}, \quad s = \frac{1}{1 - \varepsilon_1/\varepsilon_2}. \tag{1}$$

Here the positive measure μ is the spectral measure of a self-adjoint operator $\Gamma\chi$, with χ being the characteristic function of the domain occupied by one material, and $\Gamma = \nabla(-\Delta)^{-1}(\nabla\cdot)$. The spectral function μ was used to derive microstructural information about the composite [12–14], to bound the effective permittivity [10,8,15], to appraise the accuracy of the permittivity measurements [16], and to model the effective complex conductivity of geological mixtures [17,18] or of random resistor networks [19], it is calculated from reflectivity measurements at different temperatures in Ref. [20].

The present paper discusses coupling of different properties of a stationary random mixture through the spectral function μ. It is demonstrated in Ref. [6] that different properties of a random mixture admit a representation similar to Eq. (1) with the same function μ, and that the effective response of the random medium for a range of different parameters of the applied field determines the function μ. Hence, when computed from measurements of one effective property (say, from measurements of ε^*), the function μ can be used to evaluate the effective response of the same medium for other applied fields as well. From the computational point of view, the problem of reconstruction of the spectral measure μ is extremely ill-posed: It is equivalent to the inverse potential problem and requires regularization. We show computational results of recovering the spectral function μ from numerically simulated effective measurements of the complex permittivity of a second-rank composite using regularized algorithms developed in Refs. [6,22]. As an example, the thermal conductivity of St. Peters sandstone is estimated using the reconstructed function μ. We also show an example of calculation of the function μ from experimental measurements of the thermal conductivity of Berea and Tensleep sandstones [22]. Computed values of the thermal conductivity are in good agreement with measured values in Ref. [24].

2. Motivation

The knowledge of the thermal conductivity of a material is important in examining any phenomena concerning conductive heat flow. Some geophysical applications include oil reservoir simulation, high level nuclear waste containment modeling, and geothermal reservoir production simulation. Determination of the in situ distribution of thermal conductivity over a scale of meters to tens of meters using heat sources is not done typically because of the time required to diffuse a temperature field over these distances and because of the energy required for placing and maintaining calibrated heat sources. The present paper suggests an indirect approach to evaluation of the thermal conductivity of a composite medium or geological formation based on coupling of various effective properties of a composite material.

Geophysical materials are often two-scale media: Spatial variation of the complex permittivity on the large scale can be reconstructed from the measurements of the electromagnetic field on the surface and in boreholes. On a small scale, the medium is a random mixture of two components. For a two-component material such as a porous medium filled with fluid, the inverse homogenization theory suggests that the complex permittivity of the mixture, known over a broad frequency band, determines the thermal conductivity of the same composite. A coupling link between different properties of a porous medium is based on the spectral representation of the effective properties of the two-component composite medium. This indirect approach to evaluation of effective properties of a medium can be of importance in applications where direct measurements are restricted or unavailable.

3. Coupled spectral representation of effective properties of a two-component mixture

We consider a stationary random mixture of two materials with the complex permittivity ε_i and thermal conductivity k_i, $i = 1, 2$.

Theorem. *Assuming that the known properties $\varepsilon_i = \varepsilon_i(p)$, $i = 1$ or 2, of materials in a stationary random mixture depend on a parameter p, measurements of the effective complex permittivity $\varepsilon^*(p)$ in an interval $p \in (p_1, p_2)$ uniquely determine the effective thermal conductivity k^* of the mixture for given values of the components $k_i, i = 1, 2$.*

The key observation is that the effective properties ε^* and k^* are coupled through the function μ in their integral representation:

$$\varepsilon^*(s) = \varepsilon_2 - \varepsilon_2 \int_0^1 \frac{d\mu(z)}{s - z}, \quad s = \frac{1}{1 - \varepsilon_1/\varepsilon_2}, \tag{2}$$

$$k^*(s') = k_2 - k_2 \int_0^1 \frac{d\mu(z)}{s' - z}, \quad s' = \frac{1}{1 - k_1/k_2}. \tag{3}$$

If the function μ is known from the measurements of ε^*, evaluation of the effective thermal conductivity k^* reduces to a simple calculation. Indeed, let the function $F(s)$ (1) corresponding to ε^*, be represented as

$$F(s) = \sum_n \frac{\alpha_n}{s - z_n}. \tag{4}$$

The corresponding spectral function μ has the form:

$$d\mu(z) = \sum_n \alpha_n \delta(z - z_n)\, dz. \tag{5}$$

Then the effective thermal conductivity of the mixture with the thermal conductivity of the components k_1 and k_2 can be calculated as

$$k^* = k_2 \left(1 - \sum_n \frac{\alpha_n}{s' - z_n} \right) \tag{6}$$

with s' defined in Eq. (3).

It was shown in Ref. [6] that the measure μ can be uniquely reconstructed from the measurements of ε^* if the data are available on an arc in the complex plane. This is the case when the complex permittivity of one of the materials in the mixture depends on the frequency, and the measurements of the ε^* are available in a continuous interval of frequency of the applied field. Another example could be provided by a porous medium saturated with different fluids. In both cases, the materials in the mixture change their properties, but the microgeometry does not change. Transformed to the s-plane, the data points will correspond to the same function $F(s)$ with different values s belonging to some arc, $s \in \mathscr{C}$. The idea is to consider (1) as an integral equation and try to solve it and to find the corresponding function μ.

4. Ill-posedness of the problem and regularization

The problem of reconstruction of the spectral measure μ can be reduced to an inverse potential problem. The function $F(s)$ admits a representation as a logarithmic potential of the measure μ

$$F(s) = \frac{\partial}{\partial s} \int \ln |s - z|\, d\mu(z),$$
$$\partial/\partial s = (\partial/\partial x - i\partial/\partial y). \tag{7}$$

The reconstruction problem for the logarithmic potential is extremely ill-posed and requires regularization to develop a stable numerical algorithm. Let A be an operator in Eq. (7) mapping the set of measures $\mathscr{M}[0, 1]$ on the unit interval onto the set of complex potentials defined on a curve $\mathscr{C} : \zeta(s) = 0$:

$$A\mu(s) = f(s) + ig(s) = \frac{\partial}{\partial s} \int_0^1 \ln |s - z|\, d\mu(z), \quad s \in \mathscr{C}. \tag{8}$$

To construct the solution we formulate the minimization problem:

$$\|A\mu - F\| \to \min_{\mu \in \mathscr{M}}, \tag{9}$$

where $\| \cdot \|$ is the $L^2(\mathscr{C})$-norm, F is the function of the measured data, $F(s) = 1 - \varepsilon^*(s)/\varepsilon_2$, $s \in \mathscr{C}$. The solution of the problem does not continuously depend on the data: Unboundness of the operator A^{-1} leads to arbitrarily large variations in the solution, and the problem requires a regularization technique.

A regularization algorithm developed in Ref. [6] is based on constrained minimization: It introduces a stabilization functional $J(\mu)$ which constrains the set of minimizers. As a result, the solution depends continuously on the input data. Instead of minimizing (9) over all functions in $\mathcal{M}$, minimization is performed over a convex subset of functions which satisfy $J(\mu)\leqslant\beta$, for some scalar $\beta>0$. We used a quadratic stabilization functional and a total variation functional. Since the solution of the constrained minimization problem

$$\min_{\mu:\, J(\mu)\leqslant\beta} \|A\mu - F^{\delta}\| \tag{10}$$

occurs on the boundary of the constrained region where $J(\mu)=\beta$, we can reformulate (10) in terms of an unconstrained minimization problem using the Lagrange multipliers method. This approach leads to an equivalent formulation that uses the Tikhonov regularization functional $\mathcal{J}^{\alpha}(\mu,F^{\delta})$, so that problem (10) is equivalent to solving the unconstrained minimization problem with a regularization parameter α (see Ref. [23]):

$$\mathcal{J}^{\alpha}(\mu,F^{\delta}) = \|A\mu - F^{\delta}\|^2 + \alpha J(\mu),$$
$$\mathcal{J}^{\alpha}(\mu,F^{\delta}) \to \min_{\mu\in\mathcal{M}}. \tag{11}$$

The advantage of using a quadratic stabilization functional $J(\mu)=\|L\mu\|^2$, is the linearity of the corresponding Euler equation resulting in efficiency of the numerical schemes:

$$\mu_{\alpha} = (A^*A + \alpha L^*L)^{-1}A^*F^{\delta}. \tag{12}$$

However, the reconstructed solution necessarily possesses a certain smoothness. The alternative regularization based on the non-negativity constraint [21], does not impose smoothness on the solution, this permits recovering sharp features of the solution. In this approach the non-negativity of the function μ is used explicitly in the algorithm, which becomes a constrained minimization algorithm:

$$\|A\mu - F\| \to \min_{\mu\in\mathcal{M}^+}, \tag{13}$$

where $\mathcal{M}^+$ is a subset of non-negative functions on unit interval.

5. Numerical examples

5.1. Frequency dependent complex permittivity of the medium

As a first test example we consider a very simple microgeometry formed by ellipsoids of volume v with a dielectric constant ε_1 embedded in a much larger homogeneous host with a dielectric constant ε_2:

$$\varepsilon^* = \varepsilon_2 + v/V\varepsilon_2\frac{\varepsilon_1-\varepsilon_2}{\varepsilon_2 + n(\varepsilon_1-\varepsilon_2)}. \tag{14}$$

Here V is the total volume, n is depolarization factor, $n=\frac{1}{3}$ for spheres. It can be seen that ε^* diverges when $\varepsilon_1 = -(1-n)\varepsilon_2/n$, after transformation to the s-plane this gives a pole at $z_0=\frac{1}{3}$. We assume that the complex permittivity of water is given by the Debye relaxation function:

$$\varepsilon_{\rm water} = \varepsilon_{\infty} + \frac{\varepsilon_{\rm s}-\varepsilon_{\infty}}{1+{\rm i}\omega\tau}. \tag{15}$$

Here $\varepsilon_{\rm s}$ is the static dielectric constant (the value at zero frequency), ε_{∞} is the value at high frequency, $\omega=2\pi f$ is the angular frequency, with f being the frequency of the field, and τ is the relaxation time. In the present numerical example these parameters have the values: $\varepsilon_{\rm s}=80$, $\varepsilon_{\infty}=4.9$, $\tau=7.20$ ps. The second component in the mixture is assumed to have complex permittivity of sandstone, which does not vary with frequency.

Numerically simulated values of the imaginary part of the effective complex permittivity in a range of frequency were used to recover the function μ. Results of reconstruction of the spectral function μ for this example using Tikhonov regularization are shown in Fig. 1. The left figure shows solutions computed with different parameters α. Solutions calculated with too small values of regularization parameter α are shown on the right. These shown in the right figure results indicate that the problem cannot be solved without regularization. The true delta function solution at $z_0=\frac{1}{3}$, can be reconstructed almost exactly with a

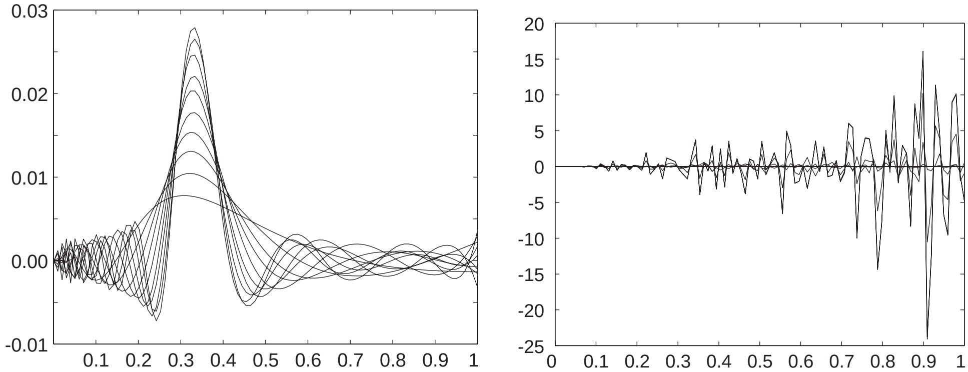

Fig. 1. Reconstruction of the spectral function using Tikhonov regularization. The true solution is a delta function at $z_0 = \frac{1}{3}$. Smooth functions on the left figure are computed with different parameters α. Solutions calculated with too small values of regularization parameter α are shown on the right.

non-negativity constraint used for regularizing this problem in Ref. [21].

5.2. Reconstruction of the spectral function for the second rank laminate

The effective complex permittivity of the second rank laminate structure shown in Fig. 2 can be calculated analytically. The corresponding function $\bar{F}(s)$ has components $F_x(s)$ and $F_y(s)$ in the directions x and y:

$$\bar{F} = \begin{pmatrix} F_x & 0 \\ 0 & F_y \end{pmatrix} = I - \frac{\varepsilon^*}{\varepsilon_2}, \quad \varepsilon^* = \begin{pmatrix} \varepsilon_x^* & 0 \\ 0 & \varepsilon_y^* \end{pmatrix}, \tag{16}$$

where the functions $F_x(s)$ and $F_y(s)$ in the s-plane are:

$$F_x(s) = m_1\left(\frac{A_1}{s-s_1} + \frac{A_2}{s-s_2}\right),$$
$$F_y(s) = m_1\left(\frac{p_2}{s} + \frac{p_1}{s-m_2}\right). \tag{17}$$

Here m_1 and m_2 are volume fractions of materials in the first rank layers, while p_1 and p_2 are volume fractions in the second rank layers. Parameters s_1, s_2 are the following:

$$s_1 = \tfrac{1}{2}(1 + \sqrt{1 - 4p_2m_1m_2}),$$
$$s_2 = \tfrac{1}{2}(1 - \sqrt{1 - 4p_2m_1m_2}) \tag{18}$$

and A_1, A_2 are given as

$$A_1 = \frac{1 - p_2m_2 - s_1}{s_2 - s_1}, \quad A_2 = \frac{1 - p_2m_2 - s_2}{s_1 - s_2}. \tag{19}$$

Numerically simulated values of ε_x^* and ε_y^* were used to calculate the spectral measures μ_x and μ_y. The results of computation using the inversion method [21] are shown in the right Fig. 2. The parameters of the laminate were taken as $m_1 = 0.2$, $m_2 = 0.8$ for the first rank layers, and $p_1 = 0.5$, $p_2 = 0.5$ for the second rank layers. The true spectral function found analytically is

$$\begin{pmatrix} \mu_x & 0 \\ 0 & \mu_y \end{pmatrix} = \begin{pmatrix} 0.12\delta(s-0.09) + 0.076\delta(s-0.91) & 0 \\ 0 & 0.1\delta(s) + 0.1\delta(s-0.8) \end{pmatrix}. \tag{20}$$

Reconstructed solution shown on the right in Fig. 2, very well identifies the support of the spectral function as well as its amplitude.

5.3. Reconstruction of the spectral function from experimental data for thermal conductivity

We applied the algorithm to reconstruction of the function μ from experimental thermal

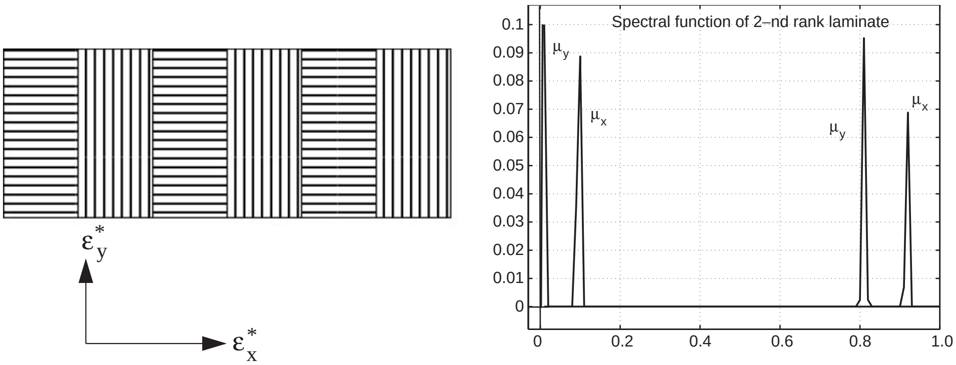

Fig. 2. The left figure shows geometry of the 2nd rank laminate. Figure on the right shows two components μ_x and μ_y of the spectral function of 2nd rank laminate reconstructed from the simulated effective comlex permittivity ε^*.

conductivity data measured in Ref. [22]. In this work the samples of various sandstone materials were saturated with different fluids with known thermal conductivity k_s. The sandstone is a random mixture of sandgrains (about 90% quartz) and saturating fluid (gas). The thermal conductivity of the quartz was assumed to be 20 mcal/cm s°C. We analyze two sets of measurements of the effective thermal conductivity k^* for Berea sandstone and for Tensleep sandstone. The data sets were very small, and one data point in both sets was far away from the rest of the measurements. We did not consider this outermost point since we did not have enough information to try to fit it in. The reconstructed spectral functions corresponding to these two data sets are shown in Fig. 3. Fig. 4 shows the original data points together with the calculated values for the effective thermal conductivity, as well as these values transformed to the s-plane. The constructed function can be used to evaluate other properties of the same sandstone by exploiting Eq. (6). Of course, the accuracy of approximating the effective behavior of composite depends on the distance of the point s' to the set of measured data points used in computation. This resolution issue will be addressed separately.

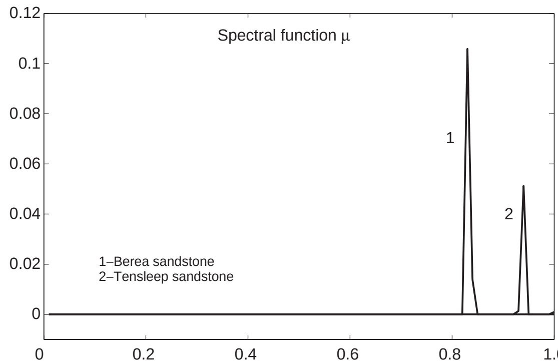

Fig. 3. The spectral function reconstructed from experimental data on the thermal conductivity of Berea and Tensleep sandstones.

5.4. Comparison with experimental data

For appraisal of the suggested indirect method of computation of the effective properties of the composite from a known effective complex permittivity, the approach was applied to the data for St. Peters sandstone, which is composed of sandgrains and has 11% porosity. Assuming the porous space is filled with water, with known dependence of $\varepsilon_{\mathrm{water}}$ on frequency, given by Eq. (15), measurements of the effective $\varepsilon^*(\omega)$ were simulated using the Maxwell–Garnett formula for a two phase composite material.

$$\varepsilon^*(\omega) = \varepsilon_{\mathrm{grain}}\left[1 - \frac{dp_{\mathrm{water}}(\varepsilon_{\mathrm{grain}} - \varepsilon_{\mathrm{water}}(\omega))}{\varepsilon_{\mathrm{grain}}(d-1) + \varepsilon_{\mathrm{water}}(\omega) + p_{\mathrm{water}}(\varepsilon_{\mathrm{grain}} - \varepsilon_{\mathrm{water}}(\omega))}\right]. \tag{21}$$

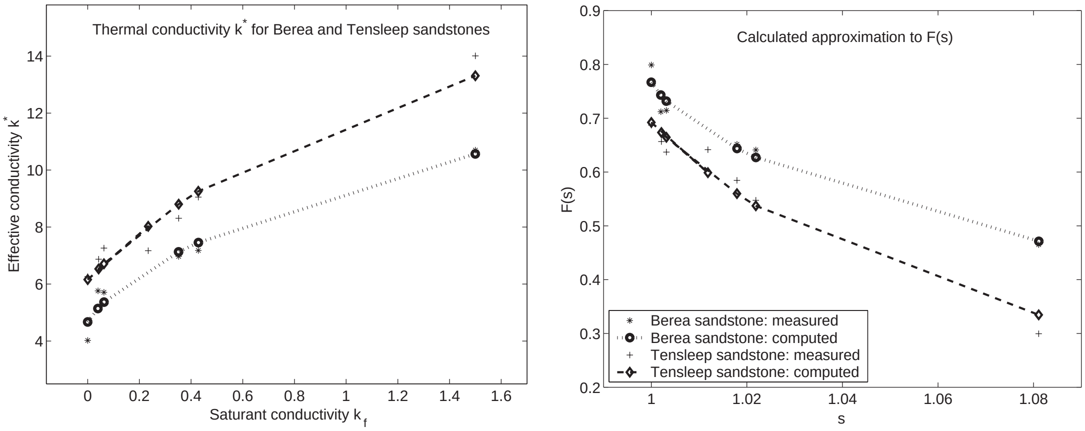

Fig. 4. The left figure shows the original measured data points together with the calculated values for the effective thermal conductivity k^*. The right figure shows the corresponding values $F(s)$ on the real axis in the s-plane which were used in calculations.

Table 1
Thermal conductivity of St. Peters sandstone

	Wet sandstone	Dry sandstone
Measured	6.36	3.56
Computed	6.63	3.55

Here d is the dimension, $d = 3$, and $p_{\text{water}} = 0.11$ is the fraction of water in the mixture. These simulated data of $\varepsilon^*(\omega)$ were used to compute the spectral function μ, which was used then to calculate the thermal conductivity of the rock. Computed and measured data for wet (sandgrains and 11% of water) and dry (sandgrains and 11% of air) sandstone are summarized in Table 1. Experimental data taken for comparison from Ref. [24] are shown as well in the table. Values of the thermal conductivity computed using the developed algorithm are in good agreement with the measured data. This comparison suggests that the method can be used for indirect evaluation of various effective properties of a random mixture computing them from measured complex permittivity or other properties of the composite.

6. Conclusion

Coupling of various effective properties of the mixture permits the use of the permittivity data to evaluate the thermal conductivity of the material. The approach might provide an alternative indirect method of evaluation of the material properties of the medium using remote electromagnetic measurements.

Acknowledgements

The authors are grateful to Alan C. Tripp for providing the thermal conductivity data and many helpful comments. This work was partially supported by DOE/OBES grant DE-FG03-93ER14313, ONR grant N0000149310141, and Schlumberger-Doll Research.

References

[1] S. Prager, J. Chem. Phys. 50 (10) (1969) 4305.
[2] A. Cherkaev, Variational Methods for Structural Optimization, Springer, New York, 2000.
[3] G.W. Milton, Theory of Composites, Cambridge Press, Cambridge, 2002.
[4] S. Torquato, Random Heterogeneous Materials. Microstructure and Macroscopic Properties, Springer, New York, 2002.
[5] M. Avellaneda, S. Torquato, Phys. Fluids A 3 (11) (1991) 2529.
[6] E. Cherkaev, In verse Problems 17 (2001) 1203.
[7] D.J. Bergman, Phys. Rep. C 43 (1978) 377.
[8] D.J. Bergman, Ann. Phys. 138 (1982) 78.
[9] G.W. Milton, Appl. Phys. Lett. 37 (3) (1980) 300.
[10] G.W. Milton, J. Appl. Phys. 52 (8) (1981) 5286.

[11] K. Golden, G. Papanicolaou, Commun. Math. Phys. 90 (1983) 473.
[12] R.C. McPhedran, D.R. McKenzie, G.W. Milton, Appl. Phys. A 29 (1982) 19.
[13] R.C. McPhedran, G.W. Milton, Mater. Res. Soc. Symp. Proc. 195 (1990) 257.
[14] E. Cherkaeva, K.M. Golden, Waves Random Media 8 (1998) 437.
[15] D.J. Bergman, SIAM, J. Appl. Math. 53 (4) (1993) 915.
[16] D. Eyre, G.W. Milton, J.V. Mantese, Phys. Rev. Lett. 79 (1997) 3062.
[17] E. Cherkaeva, A.C. Tripp, Ninth Conference of the European Consortium for Mathematics in Industry, ECMI 96, Denmark, 1996, pp. 304.
[18] A.C. Tripp, E. Cherkaeva, J. Hulen, Geophys. Prospecting 46 (6) (1998) 589.
[19] A.R. Day, M.F. Thorpe, J. Phys.: Condens. Matter 8 (1996) 4389.
[20] A.R. Day, M.F. Thorpe, A.R. Grant, A.J. Sievers, Physica B 279 (2000) 17.
[21] E. Cherkaev, P.C. Hansen, A. Berglund, Regularization using non-negativity constraints, to be published.
[22] W. Woodside, J.H. Messmer, J. Appl. Phys. 43 (9) (1961) 1699.
[23] A.N. Tikhonov, V.Y. Arsenin, Solutions of Ill-posed Problems, Wiley, New York, 1977.
[24] J.R. Hearst, P.H. Nelson, Well Logging for Physical Properties, McGraw-Hill, New York, 1985.